
THE MULTIPLE SUBNETWORK HYPOTHESIS

ENABLING MULTIDOMAIN LEARNING BY ISOLATING TASK-SPECIFIC SUBNETWORKS IN FEEDFORWARD NEURAL NETWORKS

Jacob Renn, Ian Sotnek, Benjamin Harvey

AI Squared, Inc.

United States

{jacob.renn, ian.sotnek, benjamin.harvey}@squared.ai

Brian Caffo

Department of Biostatistics

Johns Hopkins University

Baltimore, MD, USA

bcaffo1@jhu.edu

ABSTRACT

Neural networks have seen an explosion of usage and research in the past decade, particularly within the domains of computer vision and natural language processing. However, only recently have advancements in neural networks yielded performance improvements beyond narrow applications and translated to expanded multitask models capable of generalizing across multiple data types and modalities. Simultaneously, it has been shown that neural networks are overparameterized to a high degree, and pruning techniques have proved capable of significantly reducing the number of active weights within the network while largely preserving performance. In this work, we identify a methodology and network representational structure which allows a pruned network to employ previously unused weights to learn subsequent tasks. We employ these methodologies on well-known benchmarking datasets for testing purposes and show that networks trained using our approaches are able to learn multiple tasks, which may be related or unrelated, in parallel or in sequence without sacrificing performance on any task or exhibiting catastrophic forgetting.

1 Introduction

Recent advancements in deep learning have seen artificial neural networks (ANNs) match or exceed human-level performance in narrow tasks [1, 2, 3, 4]. When exposing artificial intelligence (AI) to environments that are flexible and novel, however, narrow AI loses the ability to flexibly identify and react to patterns. AI remains unable to match biological intelligence in flexibly negotiating dynamically changing environments. This is because biological learning enables the continuous acquisition of new knowledge and development of new capabilities across multiple disparate inputs, all without the newly learned information destroying internal state representations necessary to perform previously learned skills or utilize previously acquired knowledge.

The inability of a traditional ANN to learn multiple tasks across heterogeneous data sources without exhibiting catastrophic forgetting is a significant obstacle on the path to generalizable AI. Solving this challenge is a step towards enabling AI to emulate biological continuous multidomain learning; rather than relying on separate ANNs to learn and perform multiple tasks, a single neural network capable of learning multiple tasks can replicate the flexibility of human learning, simplifying the deployment of the capabilities of an AI system in dynamic, chaotic environments [5, 6].

As demonstrated in this manuscript, the training procedure described herein outputs a single neural network containing multiple subnetworks, each of which is capable of learning a single task. Practically speaking, this methodology yields a single network with the capabilities of multiple disparate networks, while also doing so more efficiently by only utilizing a small portion of the original network’s weights for each task.

2 Background

In this work, we are concerned with overcoming catastrophic forgetting in the development of ANNs capable of learning multiple tasks across disparate domains. To accomplish this, we pose and investigate the *Multiple Subnetwork Hypothesis* and build upon it to create a multitask ANN architecture capable of learning multiple tasks across various different data types and with different input and output shapes.

2.1 The Multiple Subnetwork Hypothesis

We propose the *Multiple Subnetwork Hypothesis* – that a dense, randomly-initialized feedforward ANN contains within its architecture multiple disjoint subnetworks which can be utilized together to learn and make accurate predictions on multiple tasks, regardless of the degree of similarity between tasks or input types. Additionally, we have developed the network distillation procedure *Reduction in Sub-Network Neuroplasticity* (RSN2), which optimizes

and sparsifies dense ANNs, to test our hypothesis. Our approach enables state of the art performance on multiple tasks within the same neural network without parameter overlap, and therefore without exposing subnetworks to the conditions giving rise to interference during multitask learning.

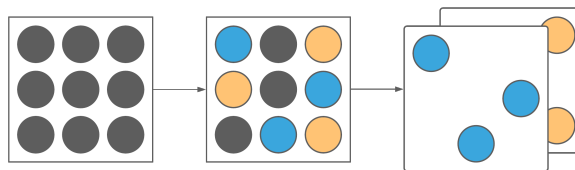


Figure 1: Illustration of the Multiple Subnetwork Hypothesis. Multiple subnetworks able to represent a fully-connected neural network for a given task are identified in a single dense, randomly-initialized feedforward neural network. These multiple specialist subnetworks can then be arrayed as a sparse tensor to isolate task representations, shielding them from catastrophic interference and enabling multi-domain task performance.

2.2 Sparse Subnetwork Identification and Isolation

It is well known and documented that ANNs are often extremely overparameterized, and this overparameterization results in redundancies and inefficiencies which can be eliminated to conserve computational resources without negatively affecting model accuracy [7]. The pruning of an ANN to reduce or eliminate extraneous parameters yields a sparse representation of the original fully-connected network, and the challenge is therefore to identify which subnetwork of parameters within a dense ANN will best represent the entire original ANN [8, 9, 10].

One means of reducing parameter count and computational requirements without sacrificing the accuracy of the sparse network is through the identification of sparse subnetworks within dense neural networks. In a randomly-initialized feed-forward network, there may be a subnetwork which can sufficiently represent the original network, called in other works a “winning lottery ticket” [11]. This methodology serves as the primary inspiration of our Multiple Subnetwork Hypothesis, as we explore in this study whether the parameters excluded from a subnetwork for one task may be utilized in the formation of subnetworks capable of learning and performing additional tasks.

2.3 Interference-Resistant Multitask Learning

Continuous learning in both biological and artificial neural systems is constrained by the stability-plasticity dilemma. Learning must be sufficiently plastic to allow the acquisition of new knowledge, but also sufficiently stable to prevent the forgetting of previous knowledge [12]. Interference stemming from lack of stability during sequen-

tial learning in ANNs, often referred to as Catastrophic Forgetting, is a result of the tendency of NNs to destroy internal state representations used in learning previously acquired tasks when learning a new task [13, 14, 15]. This phenomenon is especially pronounced in continuous learning paradigms with a low degree of inter-task relatedness [16, 17, 18], posing a challenge to creating multitask models able to perform prediction or classification across very different tasks, input data types, or input shapes. Effective mitigation of catastrophic forgetting is therefore a key prerequisite to achieving the flexibility and adaptability of a multidomain multitask artificial intelligence.

Isolating parameters for a given task, thereby fixing parameter subsets for a given task, is a means of achieving maximal stability in a continuous learning context [19]. Parameter isolation methods localize the performance of learned tasks over a physically [20, 21, 22] or logically [23, 24, 25] isolated region of an ANN, reducing or eliminating the interaction of weights responsible for a given task, therefore minimizing the opportunity for the acquisition of new tasks to interfere with the ability of an ANN to continue to perform previously learned tasks. The limitation of interactions between functional groups of neurons has its basis in the biological necessity to not only functionally integrate information in the brain, but to isolate the processing of that information into distinct modules, as evidenced by the importance of locally specialized regions in processing sensory information [26]. While the isolation of subnetworks is the surest way to prevent interference arising from learning new tasks, this method can scale poorly under memory and computational constraints and therefore demands a flexible approach to limiting network capacity [20] or minimizing the size of the network utilized for each task. Our methodology aims to negate the high computational cost of parameter isolation by applying our RSN2 methodology to represent multidomain multitask models as sparse tensors, thereby minimizing their computational footprint.

3 Methodology

In this section, we will discuss how we enable a single model to learn multiple tasks across multiple domains and datatypes through both a task-specific weight representational structure and a modified training procedure which selects disjoint subsets of network weights for each individual task.

3.1 Multitask Representational Structure

The weights of fully connected neural network layers traditionally consist of a kernel tensor, k , of shape $m \times n$, and a bias vector, b , of length n , where m denotes the number of columns in the input data and n denotes the number of neurons within the layer. To process input data \bar{x} , the decision function is thus $\Phi(k\bar{x} + b)$, where Φ denotes the layer’s activation function. Suppose then that there are inputs from two different distributions, \bar{x}_1 and \bar{x}_2 . Given the

Algorithm 1 RSN2 Training Procedure

Input: Neural Network $F(x)$, Training data for multiple tasks, $X_i, Y_i, i \in \{1, 2, \dots, N\}$
for $i \in \{1, 2, \dots, N\}$ **do**

Choose $p_i, p_i \in (0, 100)$, ensuring $\sum_{i=1}^N p_i \leq 100$
 Deactivate all weights which have been used for previous tasks

Activate all weights which have not been used for previous tasks

Select (x_i, y_i) as a subset of training data and labels for the current task

Calculate active weight gradients with respect to (x_i, y_i)

Set all inactive weight gradients to 0

Identify the quantity q_i such that $p\%$ of weight gradients with respect to (x_i, y_i) is less than q_i

Deactivate all weights with gradients less than q_i and do not allow them to train

Train the network as usual, only altering identified active weights and keeping all other weights inactive
 Save all weight values for the specified task

end for

At inference time for task i , activate only stored weights for task i and perform inference as usual

two-dimensional structure of the kernel tensor in this traditional representation, there is no way to alter the decision function given the distribution currently selected.

To address this problem, we add a new dimension, t , to the kernel tensor and the bias vector within the layer to denote which distribution or task the input data belongs to, leaving the kernel tensor with a shape of $t \times m \times n$ and transforming the bias vector into a bias matrix of shape $t \times n$. The decision function for this new layer is thus altered to that in Equation 1.

$$F(\bar{x}, i) = \Phi(k_i \bar{x} + b_i) \quad (1)$$

We take a similar approach for convolutional layers. For a two-dimensional convolutions with color channels, the kernel is of shape $s_1 \times s_2 \times c \times f$, where s_1 and s_2 denote the width and height of the convolutional filters, c represents the number of channels in the input, and f corresponds to the number of filters. The bias vector in this scenario has length f . In our multitask representation of the convolutional layer, we once more add a new dimension to the front of both the kernel tensor and the bias vector to denote the task.

3.2 Sparsification and Subnetwork Identification

While the multitask representational structure described above could theoretically be used to enable a network to learn multiple tasks as-is, it alone does not help us answer our hypothesis. Alone, this structure allows multiple networks to be combined into a single model, as the number of parameters within each layer is increased by a factor of the

number of tasks. To fully test our Multiple Subnetwork Hypothesis, we devised the RSN2 training procedure, which ensures that only one weight along the task dimension is active for all other fixed indices in multitask layers.

$$I(x) = \begin{cases} 1, & \text{if } x \neq 0 \\ 0, & \text{otherwise} \end{cases} \quad (2)$$

Mathematically, we utilize the indicator function from Equation 2 as an activation function to indicate whether an individual weight is active or inactive within a layer. Using this function, we can therefore demonstrate whether disjoint subnetworks are active for all tasks by taking the sum of the indicator function across the task dimension for all other fixed indices. If for all fixed indices, b and c , the condition present in Equation 3 holds, then each weight is only active once across all tasks, meaning the task dimension adds no additional active weights to the network layer.

$$\sum_{a=1}^t I(k_{a,b,c}) \leq 1; b, c \text{ fixed} \quad (3)$$

We utilize binary masking in our training procedure to impose these conditions. These masks therefore ensure only select weights are active during training through the bitwise multiplication of the weight value and the mask value.

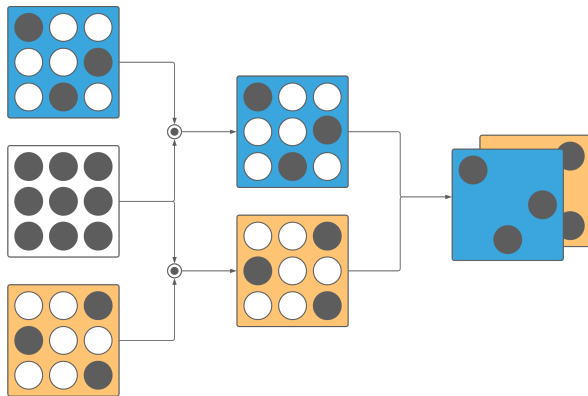


Figure 2: Diagram of the RSN2 training procedure and multitask representational structure for a single fully-connected layer with two tasks. On the left, we begin with the initialized layer weight matrix (center) and create two binary mask matrices (top and bottom). These binary masks are then bitwise-multiplied to the weight matrix, resulting in two disjoint subsets of weights which are then separated across the task dimension in our representational structure.

For weight selection and pruning, we utilize a gradient-based approach to identify which weights are to be selected for each task. By performing pruning in this manner, all pruning is done in a one-shot manner after initialization rather than iteratively as the model trains, with the pruning rate a hyperparameter selected at training time. The entirety of the RSN2 training procedure for a single network layer can be found in Algorithm 1. For performing inference, the masks used for training can be removed, thus reducing the number of active weights to a maximum value of $t * p * W$, where t represents the number of tasks, p the maximum proportion of weights active for any one task, and W the number of weights which would be present in the network had a traditional, one-task structure been used. Note that to satisfy Equation 1, $t * p \leq 1$. As a result, the RSN2 procedure, when coupled with the multitask representational structure defined above, identifies and separates disjoint subnetworks within a traditional network to allow each to individually perform separate tasks. Due to the lack of interaction between these subnetworks in the resulting model, similarity between tasks is not required, and no transfer learning will occur between tasks. A visual representation of the RSN2 training procedure and multitask representational structure can be found in Figure 2.

3.3 Experiments

We test our methodologies across eight experiments utilizing multiple datasets to test the Multiple Subnetwork Hypothesis and RSN2 training procedure. In our first experiment, we test the merits of the hypothesis by identifying whether a single network can learn the same task multiple times. To test this, we create a single convolutional multitask network and isolate five separate subnetworks within it, each utilizing a disjoint 20% of the weights within the network. Each of these subnetworks is then trained on the Fashion MNIST dataset [27]. We then compare the results of each of these subnetworks, as well as the results of the ensemble consisting of all five subnetworks, against the performance of a dedicated network with identical architecture.

Our second experiment builds upon the first by identifying if a single network can learn related tasks from a single dataset. The classes from the same Fashion MNIST dataset are broken into two groups for this experiment; the first group consists of the five individual classes which were most easily identified in the previous experiment.¹ The second group consists of the remaining five classes. The results of this experiment are compared to the performance of a dedicated network with identical architecture.

For our third experiment, we train a fully-connected network to perform both the MNIST Digit Recognition [28] and Fashion MNIST tasks and compare the performance of a single network to two dedicated networks. This ex-

¹We identified those which were learned most easily by the resulting F1 score on test data by the control model.

periment is the first we perform to test whether a single network can truly learn different tasks from multiple different domains and distributions, and it is the first experiment designed to show whether a fully connected network can perform multiple tasks.

In our fourth experiment, we train a convolutional network to perform both MNIST tasks from the previous experiment. This network is identical in architecture to all convolutional architectures trained previously, and once again this network is compared to two dedicated networks of the same architecture.

Our fifth, sixth, and seventh experiments continue to explore our hypothesis to a greater degree, as we train individual networks to perform multiple tasks across a wider array of data modalities. In the fifth experiment, we train a fully connected network to perform three tasks: both MNIST tasks as well as a regression task on house prices in the Boston area [29]. Experiment 6 trains a three-task convolutional network across both MNIST tasks as well as the CIFAR-10 dataset [30]. Our seventh and final experiment tests whether a single network can learn multiple tasks across an even wider array of input data types. For this experiment, we train a single fully-connected network to perform four tasks: both MNIST tasks, the Boston housing regression task, and an IMDB reviews sentiment classification task [31].

Our final experiment seeks to explore the feasibility of our methodologies in the context of more complicated tasks. For this experiment, we trained a single convolutional model to perform four tasks. The first three of these are the age, gender, and race prediction tasks from the UTKFace dataset [32]. The fourth task is the CIFAR10 task [30]. This experimental network is tested against four dedicated networks of identical architectures.

4 Results

In this section, we present the results for each experiment conducted. Firstly, we present the results for each control model for all tasks, as well as describe the model architectures and training schedules, as well as any data preprocessing steps which were taken. For control results, each control model was created only once and will therefore be presented with greater detail upon first presentation, but its results will be included in every pertinent experiment. For more detailed indicators of performance for all models, as well as mappings between integer labels and their respective classes, we refer the reader to the appendices.

4.1 Experiment 1: MNIST Fashion Ensemble, Convolutional Architecture

Our first experiment involved creating a single convolutional network with five disjoint subnetworks each trained on the MNIST Fashion dataset. We utilized a convolutional architecture with two convolutional blocks, with the first block containing two convolutional layers with thirty-

Table 1: Experiment 1 Results.

NETWORK	ACCURACY	PRUNING RATE
EXPERIMENTAL		
SUBNETWORK 1	90%	80%
SUBNETWORK 2	90%	80%
SUBNETWORK 3	90%	80%
SUBNETWORK 4	90%	80%
SUBNETWORK 5	92%	80%
ENSEMBLE	92%	80% EACH
CONTROL		
MNIST FASHION	92%	N/A

Table 2: Experiment 2 results.

NETWORK	ACCURACY	PRUNING RATE
EXPERIMENTAL		
EASY TASK	98%	80%
HARD TASK	84%	80%
CONTROL		
MNIST FASHION	92%	N/A

two 3×3 filters and ReLU activation [33] followed by maximum pooling over a 2×2 filter area. The second convolutional block was identical to the first, except each of the convolutional layers utilized sixty-four filters. The output to the convolutional blocks were then flattened and fed into two fully-connected layers with 256 neurons each and ReLU activation. A final fully-connected layer with ten neurons and softmax activation was used to provide the final outputs. The only preprocessing which was done on input data was a division of pixel values by 255 to ensure all input values were within the interval from 0 to 1. The model was trained using a batch size of 512, and early stopping was initialized after three epochs with no improvement of greater than 0.01 in loss on validation data. The same architecture, preprocessing steps, and training procedure was completed in the experimental case as well, with each subnetwork pruned so that 20% of the network weights were allocated to each task. A summary of results can be found in Table 1.

4.2 Experiment 2: MNIST Fashion Two-Task Model, Convolutional Architecture

For our second experiment, we utilized an identical architecture, data preprocessing, and training procedure to the previous experiment but trained two individual subnetworks within that architecture. We trained the first subnetwork on the five classes which were most easily identified by the control model, measured by F1 score, and we trained the second subnetwork on the five classes which were the most difficult for the control model to identify, also measured by F1 score. The results of the experiment can be found in Table 2.

Table 3: Experiment 3 results.

NETWORK	ACCURACY	PRUNING RATE
EXPERIMENTAL		
MNIST DIGIT	97%	90%
MNIST FASHION	86%	90%
CONTROL		
MNIST DIGIT	97%	N/A
MNIST FASHION	88%	N/A

Table 4: Experiment 4 results.

NETWORK	ACCURACY	PRUNING RATE
EXPERIMENTAL		
MNIST DIGIT	99%	80%
MNIST FASHION	90%	80%
CONTROL		
MNIST DIGIT	99%	N/A
MNIST FASHION	92%	N/A

4.3 Experiment 3: MNIST Digits and MNIST Fashion Model, Fully-Connected Architecture

Our third experiment is the first experiment to truly test whether a single model can learn disparate tasks across a variety of data modalities. To do this, we trained a single fully-connected network to perform both the MNIST Digit Recognition and the MNIST Fashion Recognition tasks. For this experiment, we preprocessed the data for both tasks once more by dividing each pixel value by 255. Each image was then flattened into a two-dimensional vector. The images would then be passed through six fully connected layers each containing 1000 artificial neurons each and activated using the ReLU activation function. The final layer contained ten neurons which were activated with the softmax activation function. The model was trained with the same early stopping conditions as all previous models, and a batch size of 512 was used once more. The experimental model was trained using the same procedure and with the same architecture, with each task pruned to utilize 10% of the network weights. The results of this experiment can be found in Table 3.

4.4 Experiment 4: MNIST Digit and MNIST Fashion Model, Convolutional Architecture

In experiment four, we repeated the modeling goals of the previous experiment, but this experiment utilized the convolutional architecture from the previous experiments, once again with an 80% pruning rate for each task. Results for this experiment can be found in Table 4.

Table 5: Experiment 5 results. In the performance column, percentages correspond to accuracy percentage on test data, while decimals represent mean squared error on test data.

NETWORK	PERFORMANCE	PRUNING RATE
EXPERIMENTAL		
MNIST DIGIT	97%	90%
MNIST FASHION	87%	90%
BOSTON HOUSING	0.016	90%
CONTROL		
MNIST DIGIT	97%	N/A
MNIST FASHION	88%	N/A
BOSTON HOUSING	0.017	N/A

4.5 Experiment 5: MNIST Digit, MNIST Fashion, and Boston Housing Model, Fully-Connected Architecture

The fifth experiment provides the greatest test for our Multiple Subnetwork Hypothesis up to this point, as we train a model with a wider variety of datatypes and tasks, and we also train some tasks in sequence rather than all at once. For this experiment, we trained a single fully-connected network first on both MNIST tasks, then trained the same network on the Boston Housing dataset. The MNIST portions of the network were identical in architecture to the ones used in previous experiments, but due to difference in input shapes between the MNIST images and the Boston Housing dataset² an additional fully-connected layer is added after the Boston Housing input layer to create shape alignment. This layer is activated with ReLU activation, and it is also pruned in the experimental model. In the test case, all subnetworks are pruned to only use 10% of available weights.

Data preprocessing for MNIST tasks is identical to previous MNIST preprocessing for fully-connected networks. For the Boston Housing dataset, input features were scaled such that the minimum feature value in the training data corresponded to a value of 0 and the maximum value of the feature in the training data corresponded to a value of 1. The predicted values were also scaled using the same procedures. During training, as stated before, both MNIST tasks are learned simultaneously, utilizing the same early stopping criteria and batch sizes as the previous cases. For the Boston Housing task, the same early stopping procedure is used, but the batch size is decreased to 32 in both the control and test cases due to the limited amount of data available. The results for this experiment can be found in Table 5.

Furthermore, to identify whether any forgetting occurred after sequential training, we recorded loss values on test data for current and previously-trained tasks after each subsequent task was trained. These results are visualized

²The MNIST images are both 28 pixels wide and 28 pixels tall, while the Boston Housing dataset contains only 13 input features.

in Figure 3, where it can be seen that no performance degradation occurred on the first two tasks after training the third task.

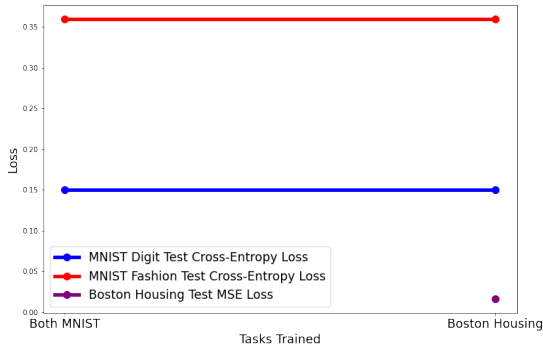


Figure 3: Task losses obtained on test data for multitask model after training each set of tasks.

4.6 Experiment 6: CIFAR10, MNIST Digit, and MNIST Fashion Model, Convolutional Architecture

Experiment 6 was designed to expand upon the findings of previous experiments by testing whether a single convolutional network could converge across multiple classification tasks across a variety of input images. In this experiment, we test whether a single convolutional network can converge on first the CIFAR-10 image classification task and then train the same network on both MNIST tasks we have utilized to this point. To ensure that all images are of the same shape, we downsize the CIFAR-10 images so that they have the same height and width as the MNIST data. Additionally, because of the color channels present in the CIFAR images, a separate first convolutional layer must be created to process the CIFAR-10 inputs in the multitask model. This dedicated layer is still pruned to the same degree as all other processing layers within the model. During training, the same early stopping procedures that have been used previously were employed, and batch sizes of 512 were used for all tasks. The results for this experiment can be found in Table 6, and task losses after training can be found in Figure 4. The test model was pruned to 90% in this experiment.

4.7 Experiment 7: MNIST Digit, MNIST Fashion, Boston Housing, and IMDB Reviews Model, Fully-Connected Architecture

Our seventh experiment provides perhaps the most wide-ranging set of tasks for a single network, and as a result it is perhaps the best test of our Multiple Subnetwork Hypothesis. In this experiment, we utilized a single fully-connected neural network and trained the network on four

Table 6: Experiment 6 results.

NETWORK	ACCURACY	PRUNING RATE
EXPERIMENTAL		
CIFAR-10	60%	80%
MNIST DIGIT	98%	90%
MNIST FASHION	89%	90%
CONTROL		
CIFAR-10	47%	N/A
MNIST DIGIT	99%	N/A
MNIST FASHION	92%	N/A

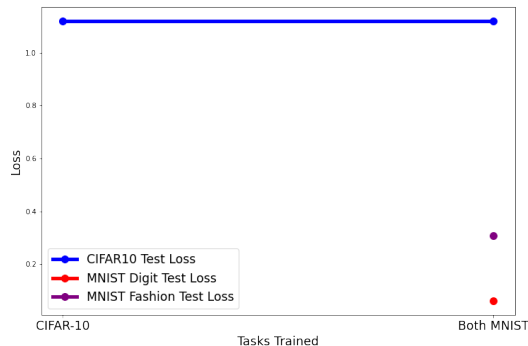


Figure 4: Task losses obtained on test data for multitask model after training each set of tasks.

separate tasks; the first two of these tasks, both the MNIST Digit and MNIST Fashion tasks, were trained simultaneously. The third task, the Boston Housing regression task, was then trained. Finally, the IMDB reviews sentiment classification task was trained. The same architecture as previously used in all fully-connected experiments was used in this experiment. For the MNIST and Boston Housing tasks, the same preprocessing and reshaping efforts took place as previous experiments with fully-connected architectures. For the IMDB task, only the most common 10000 words were utilized and sequences were padded (or truncated) to 128 words, with both padding and truncating occurring at the end of the review. Furthermore, each of the input tokens was passed through an embedding layer, which embedded the token in a two-dimensional vector space. The embedded tensors were then flattened into a two-dimensional vector and passed through the architecture used throughout this experiment³. For the multitask model in this experiment, the first fully-connected layer which processed inputs from the IMDB task was dedicated solely to the IMDB task due to the differences in input shapes between all tasks. During training, the same early stopping criteria were used for all training iterations, batches sizes of 512 were used for the MNIST and IMDB

³This architecture involves six fully-connected layers of 1000 neurons and ReLU activation.

Table 7: Experiment 7 results. In the performance column, percentages correspond to accuracy percentage on test data, while decimals represent mean squared error on test data.

NETWORK	PERFORMANCE	PRUNING RATE
EXPERIMENTAL		
MINST DIGIT	97%	90%
MNIST FASHION	87%	90%
BOSTON HOUSING	0.011	90%
IMDB	82%	90%
CONTROL		
MNIST DIGIT	97%	N/A
MNIST FASHION	88%	N/A
BOSTON HOUSING	0.017	N/A
IMDB	80%	N/A

tasks, while a batch size of 32 was used for the Boston Housing task. The results for this experiment can be found in Table 7, and task losses can be found in Figure 5. The model was pruned such that each task utilizes 10% of the available weights in fully-connected layers; the embedding layer was not pruned.

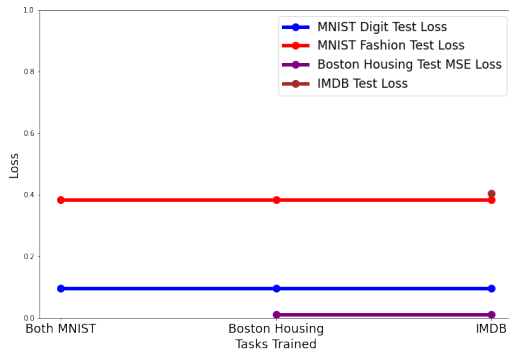


Figure 5: Task losses obtained on test data for multitask model after training each set of tasks.

4.8 Experiment 8: UTKFace and CIFAR10 Four-Task Model, Convolutional Architecture

In our final experiment, we tested the RSN2 training procedure on a larger network with more complex tasks involved. We created a single network with a convolutional architecture on four individual tasks, three tasks from the UTKFace dataset [32] and one multiclass classification task from CIFAR10 [30]. For the age task in the UTKFace data, we grouped values into classes by decade, excluding a final class containing all individuals with age greater than 90.

Architecturally, the model trained in this experiment contains three convolutional blocks containing of 16, 32, and 64 3×3 filters, respectively. Each block contains two convolutional layers with padding to preserve shape, followed

Table 8: Experiment 8 results.

NETWORK	ACCURACY	PRUNING RATE
EXPERIMENTAL		
UTKFACE AGE	55%	75%
UTKFACE GENDER	89%	75%
UTKFACE RACE	77%	75%
CIFAR10	50%	75%
CONTROL		
UTKFACE AGE	32%	N/A
UTKFACE GENDER	48%	N/A
UTKFACE RACE	14%	N/A
CIFAR10	10%	N/A

by a max pooling layer. These blocks then feed into a fully connected architecture of three layers, each with 128 neurons each and activated using ReLU activation [33], followed by an output layer of the required shape to perform the specified task.

For the multitask model, we utilized a shared convolutional embedding between all UTKFace tasks. This resulted in a two-task structure for convolutional layers within the model, with one task channel processing the UTKFace images and the other task channel processing the CIFAR10 images. For the fully-connected layers, each of the UTKFace tasks was isolated and a four-task architecture was used. Along both the convolutional and the fully-connected architectures, each task was pruned to utilize only 25% of the model’s available weights per task, meaning 50% of the weights in the convolutional layers were utilized⁴ and 100% of the weights across the shared fully-connected architecture was utilized.⁵ All four tasks were trained simultaneously, with early stopping criteria utilized with patience of five epochs. A summary of the results of this experiment can be found in 8. In addition to these performance results, which interestingly showed that the dedicated control models were unable to converge but that the multitask model was able to converge, it was also found that the multitask model only utilized 130MB of disk space when saved, while the combined single-task models utilized 203MB of disk space, over 56% more than the multitask model.

5 Discussion

This study was designed to provide insight into answering our Multiple Subnetwork Hypothesis, which states that a dense, randomly-initialized feedforward neural network contains within its architecture multiple disjoint subnetworks which can be isolated to each separately learn and make accurate predictions on multiple tasks, regardless of the degree of similarity between tasks or input types. To

⁴This is due to the two-task structure of the convolutional layers, as mentioned above.

⁵This is due to the four-task structure of the fully-connected layers, as mentioned above.

test this hypothesis, we developed the RSN2 procedure as well as a customized neural network representational structure designed to isolate individual subnetworks within the overall architecture of the global model on a layer-by-layer basis. We then utilized these techniques in a series of seven experiments across a range of datasets utilizing both fully-connected and convolutional architectures.

Across each of these experiments, we consistently saw that a single network was able to converge on multiple tasks by utilizing only a small fraction of network weights for each task. Furthermore, multitask models were able to perform each task with near identical performance to dedicated models with all weights active, even exceeding dedicated model performance in a few cases. Additionally, we saw that there needed to be no similarity between tasks, as in our most extreme case we were able to teach a single model to perform two separate image classification tasks, a tabular regression task, and a sentiment classification task on natural language.

The beneficial implications of this approach arise from the simplicity of interacting with a single model rather than a collection of models as in the traditional machine learning deployment paradigm. Take for example the human visual system: a unified stream of visual information is collected and passed to the optic lobe, where it is then passed to the relevant regions of the brain for further downstream analysis. This paradigm is reflected in the unified data pipeline of a multitask model trained using the RSN2 procedure, where invoking the model involves invoking the relevant task or tasks automatically. Therefore, a collection of models capable of performing multiple tasks can be deployed as a single entity within an organization’s IT infrastructure, thereby improving efficiency and lowering costs. Take, for instance, a simple example of an organization which wants to deploy five separate models trained on five separate tasks. A typical deployment scenario would involve this organization deploying one model each to five separate computational nodes. Using a model trained with the RSN2 procedure to perform all five tasks, this organization could therefore reduce costs by deploying this single multitask model to a single node, saving 80% of the organization’s original costs. Furthermore, to improve system robustness by introducing redundancy, the organization could deploy this single model to a set of three nodes and still reduce costs by 40%.

Additionally, in our final experiment, even though we do not utilize sparse tensors to save the model, the pruned multitask model utilizes less disk space when saved compared to the total amount of the identical single-task models. This indicates that utilizing RSN2 and our multitask representational structure already leads to more efficient representation of the models themselves, thus potentially further reducing costs by decreasing the hardware requirements needed to save and use models for inference.

5.1 Limitations

There are a number of limitations to this study which limit the conclusions we can draw from the results. Firstly, our experiments focus primarily on computer vision related tasks in this work, with all experiments containing some image classification task. While we do also include experiments which test our methods on both tabular input and natural language inputs, further studies should still be conducted to more rigorously test our hypotheses and methods on various input and data types.

Another limitation to this study is the limited size of both the datasets and models which were studied. Many state of the art models have been trained on millions of data samples, and the models themselves consist of many tens of millions of parameters. Our study, on the other hand, considered labeled data with up to tens of thousands of samples and models which contained hundreds of thousands to millions of parameters, orders of magnitude fewer (in both cases) than the state of the art in most cases. It is therefore unknown whether these methods would need to be modified⁶ to accommodate larger modeling paradigms.

5.2 Conclusions

Despite the limitations to this study, there are still a number of conclusions we can draw from its results. Each multitask model was clearly able to converge on all its assigned tasks, achieving performance similar to, and in some cases exceeding, the control cases each time. These results therefore confirm our Multiple Subnetwork Hypothesis, showing that a single neural architecture is capable of utilizing small portions of itself to learn individual tasks. Additionally, we showed that our methodology for identifying and logically separating network weights is robust to catastrophic forgetting, and we showed that we were therefore able to train multitask models across various domains and tasks both in parallel or in sequence without any adverse effects on previously-learned tasks.

Because the resulting model would have the ability to robustly perform multiple tasks, we can also conclude that a single model trained with these techniques could substitute multiple models in a deployed scenario. This substitution would therefore reduce resource requirements for organizations deploying and utilizing models, thus saving costs and simplifying the deployment architectures these organizations use. These models would also be able to acquire more downstream tasks after previously being trained on initial tasks, meaning adding new predictive analytics would be a much simpler undertaking as well, as it would only involve updating an already-deployed model and not require creating a completely new deployment for every new analytic.

⁶In particular, it is unknown whether our one-shot sparsification technique would generalize to much larger models.

5.3 Future Work

Following studies should be designed to address some of the limitations of this work as well as to improve the methods used within. Future studies should provide a more thorough analysis on how these methods perform on a larger variety of data modalities, including data types, task types, data availability, and model sizes. Secondly, we intend to identify whether a more precise pruning method can be applied as training occurs instead of in a one-shot manner as was done in this study. If pruning can be applied in a more intelligent manner, we believe the resulting model would potentially be able to more consistently surpass unpruned model performance while also achieving greater sparsification rates than possible with one-shot techniques.

Additionally, this study does not perform any analysis to identify the maximum amount of tasks which can be learned by a single network. Future work should therefore address finding the upper bounds of the number of tasks an individual model can support. Finally, the methods in this work do not allow for any transfer learning across tasks; instead, it is assumed that new tasks should utilize a completely disjoint subset of weights relative to all previously-learned tasks. Additional studies should be conducted to identify whether transfer learning can be leveraged during the acquisition of similar tasks to enable further reduction in the number of active weights and the quicker acquisition of new tasks.

References

- [1] Kumar Chellapilla, Kevin Larson, Patrice Simard, and Mary Czerwinski. Computers beat humans at single character recognition in reading based human interaction proofs (hips). 01 2005.
- [2] David Silver, Aja Huang, Chris J. Maddison, Arthur Guez, Laurent Sifre, George van den Driessche, Julian Schrittwieser, Ioannis Antonoglou, Veda Panneershelvam, Marc Lanctot, Sander Dieleman, Dominik Grewe, John Nham, Nal Kalchbrenner, Ilya Sutskever, Timothy Lillicrap, Madeleine Leach, Koray Kavukcuoglu, Thore Graepel, and Demis Hassabis. Mastering the game of go with deep neural networks and tree search. *Nature*, 529(7587):484–489, 2016.
- [3] Murray Campbell, A. Joseph Hoane, and Feng hsiung Hsu. Deep blue. *Artificial Intelligence*, 134(1):57–83, 2002.
- [4] Oriol Vinyals, Igor Babuschkin, Wojciech M. Czarnecki, Michaël Mathieu, Andrew Dudzik, Junyoung Chung, David H. Choi, Richard Powell, Timo Ewalds, Petko Georgiev, Junhyuk Oh, Dan Horgan, Manuel Kroiss, Ivo Danihelka, Aja Huang, Laurent Sifre, Trevor Cai, John P. Agapiou, Max Jaderberg, Alexander S. Vezhnevets, Rémi Leblond, Tobias Pohlen, Valentin Dalibard, David Budden, Yury Sulsky, James Molloy, Tom L. Paine, Caglar Gulcehre, Ziyu Wang, Tobias Pfaff, Yuhuai Wu, Roman Ring, Dani Yogatama, Dario Wünsch, Katrina McKinney, Oliver Smith, Tom Schaul, Timothy Lillicrap, Koray Kavukcuoglu, Demis Hassabis, Chris Apps, and David Silver. Grandmaster level in starcraft ii using multi-agent reinforcement learning. *Nature*, 575(7782):350–354, 2019.
- [5] Claudine Badue, Ranik Guidolini, Raphael Vivacqua Carneiro, Pedro Azevedo, Vinicius Brito Cardoso, Avelino Forechi, Luan Ferreira Reis Jesus, Rodrigo Ferreira Berriel, Thiago Meireles Paixão, Filipe Wall Mutz, Thiago Oliveira-Santos, and Alberto Ferreira de Souza. Self-driving cars: A survey. *CoRR*, abs/1901.04407, 2019.
- [6] Zhen Qin, Yicheng Cheng, Zhe Zhao, Zhe Chen, Donald Metzler, and Jingzheng Qin. *Multitask Mixture of Sequential Experts for User Activity Streams*, page 3083–3091. Association for Computing Machinery, New York, NY, USA, 2020.
- [7] Yann LeCun, John Denker, and Sara Solla. Optimal brain damage. In D. Touretzky, editor, *Advances in Neural Information Processing Systems*, volume 2. Morgan-Kaufmann, 1990.
- [8] Kenji Suzuki, Isao Horiba, and Noboru Sugie. A simple neural network pruning algorithm with application to filter synthesis. *Neural processing letters*, 13(1):43–53, 2001.
- [9] Song Han, Huizi Mao, and William J Dally. Deep compression: Compressing deep neural networks with pruning, trained quantization and huffman coding. *arXiv preprint arXiv:1510.00149*, 2015.
- [10] Mieszko Lis, Maximilian Golub, and Guy Lemieux. Full deep neural network training on a pruned weight budget. *Proceedings of Machine Learning and Systems*, 1:252–263, 2019.
- [11] Jonathan Frankle and Michael Carbin. The lottery ticket hypothesis: Finding sparse, trainable neural networks, 2019.
- [12] Martial Mermillod, Aurélie Bugaiska, and Patrick Bonin. The stability-plasticity dilemma: Investigating the continuum from catastrophic forgetting to age-limited learning effects. *Frontiers in psychology*, 4:504, 2013.
- [13] Robert French. Catastrophic forgetting in connectionist networks. *Trends in cognitive sciences*, 3:128–135, 05 1999.
- [14] Ian J Goodfellow, Mehdi Mirza, Da Xiao, Aaron Courville, and Yoshua Bengio. An empirical investigation of catastrophic forgetting in gradient-based neural networks. *arXiv preprint arXiv:1312.6211*, 2013.
- [15] Benedikt Pfühl and Alexander Gepperth. A comprehensive, application-oriented study of catastrophic forgetting in dnns. *arXiv preprint arXiv:1905.08101*, 2019.
- [16] Rahaf Aljundi, Punarjay Chakravarty, and Tinne Tuytelaars. Expert gate: Lifelong learning with a network of experts. In *Proceedings of the IEEE Conference on Computer Vision and Pattern Recognition*, pages 3366–3375, 2017.
- [17] Jiaqi Ma, Zhe Zhao, Xinyang Yi, Jilin Chen, Lichan Hong, and Ed H Chi. Modeling task relationships in multi-task learning with multi-gate mixture-of-experts. In *Proceedings of the 24th ACM SIGKDD International Conference on Knowledge Discovery & Data Mining*, pages 1930–1939, 2018.
- [18] Marc Masana, Tinne Tuytelaars, and Joost van de Weijer. Ternary feature masks: zero-forgetting for task-incremental learning. In *Proceedings of the IEEE/CVF Conference on Computer Vision and Pattern Recognition*, pages 3570–3579, 2021.
- [19] Matthias Delange, Rahaf Aljundi, Marc Masana, Sarah Parisot, Xu Jia, Ales Leonardis, Greg Slabaugh, and Tinne Tuytelaars. A continual learning survey: Defying forgetting in classification tasks. *IEEE Transactions on Pattern Analysis and Machine Intelligence*, 2021.

- [20] Jaehong Yoon, Eunho Yang, Jeongtae Lee, and Sung Ju Hwang. Lifelong learning with dynamically expandable networks. *arXiv preprint arXiv:1708.01547*, 2017.
- [21] Andrei A Rusu, Neil C Rabinowitz, Guillaume Desjardins, Hubert Soyer, James Kirkpatrick, Koray Kavukcuoglu, Razvan Pascanu, and Raia Hadsell. Progressive neural networks. *arXiv preprint arXiv:1606.04671*, 2016.
- [22] Arun Mallya and Svetlana Lazebnik. Packnet: Adding multiple tasks to a single network by iterative pruning. In *Proceedings of the IEEE conference on Computer Vision and Pattern Recognition*, pages 7765–7773, 2018.
- [23] Xialei Liu, Marc Masana, Luis Herranz, Joost Van de Weijer, Antonio M Lopez, and Andrew D Bagdanov. Rotate your networks: Better weight consolidation and less catastrophic forgetting. In *2018 24th International Conference on Pattern Recognition (ICPR)*, pages 2262–2268. IEEE, 2018.
- [24] Joan Serra, Didac Suris, Marius Miron, and Alexandros Karatzoglou. Overcoming catastrophic forgetting with hard attention to the task. In *International Conference on Machine Learning*, pages 4548–4557. PMLR, 2018.
- [25] Arun Mallya, Dillon Davis, and Svetlana Lazebnik. Piggyback: Adapting a single network to multiple tasks by learning to mask weights. In *Proceedings of the European Conference on Computer Vision (ECCV)*, pages 67–82, 2018.
- [26] Elizabeth Zavitz and Nicholas SC Price. Understanding sensory information processing through simultaneous multi-area population recordings. *Frontiers in neural circuits*, 12:115, 2019.
- [27] Han Xiao, Kashif Rasul, and Roland Vollgraf. Fashion-mnist: a novel image dataset for benchmarking machine learning algorithms, 2017. cite arxiv:1708.07747Comment: Dataset is freely available at <https://github.com/zalando-research/fashion-mnist> Benchmark is available at <http://fashion-mnist.s3-website-eu-central-1.amazonaws.com/>.
- [28] Yann LeCun and Corinna Cortes. MNIST handwritten digit database. <http://yann.lecun.com/exdb/mnist/>, 2010.
- [29] David Harrison and Daniel L Rubinfeld. Hedonic housing prices and the demand for clean air. *Journal of Environmental Economics and Management*, 5(1):81–102, 1978.
- [30] Alex Krizhevsky, Vinod Nair, and Geoffrey Hinton. Cifar-10 (canadian institute for advanced research).
- [31] Andrew L. Maas, Raymond E. Daly, Peter T. Pham, Dan Huang, Andrew Y. Ng, and Christopher Potts. Learning word vectors for sentiment analysis. In *Proceedings of the 49th Annual Meeting of the Association for Computational Linguistics: Human Language Technologies*, pages 142–150, Portland, Oregon, USA, June 2011. Association for Computational Linguistics.
- [32] Zhifei Zhang, Yang Song, and Hairong Qi. Age progression/regression by conditional adversarial autoencoder. In *IEEE Conference on Computer Vision and Pattern Recognition (CVPR)*. IEEE, 2017.
- [33] Abien Fred Agarap. Deep learning using rectified linear units (relu). *arXiv preprint arXiv:1803.08375*, 2018.

A Class labels for classification tasks.

Table 9: Class labels for computer vision tasks.

DATASET	INTEGER	LABEL
<hr/>		
MNIST DIGIT		
	1	DIGIT “0”
	2	DIGIT “1”
	3	DIGIT “2”
	4	DIGIT “3”
	5	DIGIT “4”
	6	DIGIT “5”
	7	DIGIT “6”
	8	DIGIT “7”
	9	DIGIT “8”
	10	DIGIT “9”
<hr/>		
MNIST FASHION		
	1	T-SHIRT/TOP
	2	TROUSER
	3	PULLOVER
	4	DRESS
	5	COAT
	6	SANDAL
	7	SHIRT
	8	SNEAKER
	9	BAG
	10	ANKLE BOOT
<hr/>		
CIFAR-10		
	1	AIRPLANE
	2	AUTOMOBILE
	3	BIRD
	4	CAT
	5	DEER
	6	DOG
	7	FROG
	8	HORSE
	9	SHIP
	10	TRUCK
<hr/>		
UTKFACE AGE		
	1	0 – 10
	2	11 – 20
	3	21 – 30
	4	31 – 40
	5	41 – 50
	6	51 – 60
	7	61 – 70
	8	71 – 80
	9	81 – 90
	10	91+
<hr/>		
UTKFACE GENDER		
	1	MALE
	2	FEMALE
<hr/>		
UTKFACE ETHNICITY		
	1	WHITE
	2	BLACK
	3	ASIAN
	4	INDIAN
	5	“OTHER” ⁷

⁷Defined by dataset creators and includes ethnicities such as Hispanic, Latino, and Middle Eastern.

Table 10: Class labels for IMDB task.

INTEGER	LABEL
1	NEGATIVE REVIEW
2	POSITIVE REVIEW

B Additional model performance metrics.

When conducting our study, we collected additional performance measures for all models which were not included in the main manuscript above. These metrics are presented in the following tables.

Table 11: Per-class F1 and overall accuracy scores for control computer vision models. “FC” indicates fully-connected architecture. “Conv” indicates convolutional architecture.

NETWORK	CLASS NUMBER										ACCURACY
	1	2	3	4	5	6	7	8	9	10	
MNIST DIGIT FC	0.98	0.99	0.97	0.97	0.98	0.97	0.98	0.97	0.96	0.96	0.97
MNIST DIGIT CONV	0.99	0.99	0.98	0.99	0.99	0.99	0.99	0.99	0.99	0.98	0.99
MNIST FASHION FC	0.84	0.98	0.79	0.88	0.79	0.97	0.69	0.95	0.97	0.96	0.88
MNIST FASHION CONV	0.85	0.99	0.87	0.92	0.86	0.98	0.76	0.97	0.99	0.97	0.92
CIFAR-10 CONV (EXP 6)	0.55	0.59	0.35	0.26	0.38	0.39	0.51	0.53	0.55	0.52	0.47
UTKFACE AGE CONV	0.00	0.00	0.49	0.00	0.00	0.00	0.00	0.00	0.00	0.00	0.32
UTKFACE GENDER CONV	0.00	0.64	N/A	N/A	N/A	N/A	N/A	N/A	N/A	N/A	0.48
UTKFACE ETHNICITY CONV	0.00	0.00	0.25	0.00	0.00	N/A	N/A	N/A	N/A	N/A	0.14
CIFAR-10 CONV (EXP 8)	0.00	0.00	0.00	0.00	0.00	0.18	0.00	0.00	0.00	0.00	0.10

Table 12: Per-class F1 and overall accuracy scores for experimental computer vision models.

NETWORK	CLASS NUMBER										ACCURACY
	1	2	3	4	5	6	7	8	9	10	
EXPERIMENT 1											
SUBNETWORK 1	0.86	0.98	0.85	0.90	0.84	0.98	0.72	0.96	0.97	0.97	0.90
SUBNETWORK 2	0.85	0.97	0.84	0.89	0.83	0.98	0.72	0.96	0.98	0.96	0.90
SUBNETWORK 3	0.84	0.98	0.82	0.88	0.83	0.98	0.72	0.96	0.97	0.97	0.90
SUBNETWORK 4	0.85	0.98	0.84	0.90	0.84	0.98	0.72	0.96	0.98	0.97	0.90
SUBNETWORK 5	0.87	0.99	0.88	0.91	0.88	0.98	0.78	0.96	0.98	0.97	0.92
ENSEMBLE	0.87	0.98	0.87	0.91	0.86	0.98	0.76	0.97	0.98	0.97	0.92
EXPERIMENT 2											
EASIER TASK SUBNETWORK	N/A	1.00	N/A	N/A	N/A	0.97	N/A	0.96	0.99	0.96	0.98
HARDER TASK SUBNETWORK	0.85	N/A	0.87	0.92	0.85	N/A	0.73	N/A	N/A	N/A	0.84
EXPERIMENT 3											
MNIST DIGIT	0.99	0.99	0.98	0.97	0.97	0.97	0.98	0.98	0.97	0.96	0.98
MNIST FASHION	0.82	0.97	0.77	0.87	0.79	0.96	0.62	0.94	0.97	0.95	0.87
EXPERIMENT 4											
MNIST DIGIT	0.99	0.99	0.99	0.99	0.99	0.99	0.99	0.99	0.98	0.98	0.99
MNIST FASHION	0.85	0.98	0.85	0.90	0.85	0.98	0.71	0.96	0.97	0.96	0.90
EXPERIMENT 5											
MNIST DIGIT	0.98	0.99	0.97	0.97	0.97	0.97	0.97	0.98	0.97	0.96	0.97
MNIST FASHION	0.82	0.98	0.78	0.88	0.78	0.95	0.68	0.94	0.96	0.95	0.87
EXPERIMENT 6											
MNIST DIGIT	0.98	0.99	0.98	0.98	0.98	0.98	0.98	0.98	0.98	0.97	0.98
MNIST FASHION	0.84	0.98	0.83	0.89	0.83	0.97	0.70	0.95	0.97	0.96	0.89
CIFAR-10	0.65	0.72	0.46	0.43	0.49	0.49	0.69	0.70	0.70	0.69	0.60
EXPERIMENT 7											
MNIST DIGIT	0.98	0.99	0.98	0.96	0.97	0.96	0.97	0.96	0.96	0.96	0.97
MNIST FASHION	0.82	0.97	0.78	0.87	0.78	0.95	0.64	0.93	0.95	0.95	0.87
EXPERIMENT 8											
UTKFACE AGE	0.89	0.45	0.68	0.37	0.14	0.44	0.34	0.29	0.45	0.08	0.55
UTKFACE GENDER	0.90	0.88	N/A	N/A	N/A	N/A	N/A	N/A	N/A	N/A	0.89
UTKFACE ETHNICITY	0.84	0.83	0.79	0.68	0.27	N/A	N/A	N/A	N/A	0.77	
CIFAR-10	0.58	0.63	0.27	0.35	0.44	0.47	0.53	0.54	0.61	0.52	0.50

Table 13: Per-class F1 and overall accuracy scores for experimental and control IMDB sentiment analysis models.

NETWORK	CLASS NUMBER		ACCURACY
	1	2	
EXPERIMENT 7 IMDB	0.83	0.81	0.82
CONTROL IMDB	0.80	0.80	0.80

Table 14: Boston Housing model losses.

NETWORK	Loss
EXPERIMENT 5	0.016
EXPERIMENT 7	0.011
CONTROL	0.017